

Synthesis and Degradation of Nucleic Acid Components by Formamide and Iron Sulfur Minerals

Raffaele Saladino,^{*,†} Veronica Neri,[†] Claudia Crestini,[‡] Giovanna Costanzo,[§] Michele Graciotti,^{||} and Ernesto Di Mauro^{*,||}

Dipartimento di Agrobiologia ed Agrochimica, Università della Tuscia, Viterbo, Italy, Dipartimento di Scienze e Tecnologie Chimiche, Università Tor Vergata, Roma 00100, Italy, Istituto di Biologia e Patologia Molecolari, CNR, Roma, Italy, and Dipartimento di Genetica e Biologia Molecolari, Università "Sapienza", Roma 00185, Italy

Received June 23, 2008; E-mail: saladino@unitus.it; Ernesto.dimauro@uniroma1.it

Abstract: We describe the one-pot synthesis of a large panel of nucleic bases and related compounds from formamide in the presence of iron sulfur and iron–copper sulfur minerals as catalysts. The major products observed are purine, 1*H*-pyrimidinone, isocytosine, adenine, 2-aminopurine, carbodiimide, urea, and oxalic acid. Isocytosine and 2-aminopurine may recognize natural nucleobases by Watson–Crick and reverse Watson–Crick interactions, thus suggesting novel scenarios for the origin of primordial nucleic acids. Since the major problem in the origin of informational polymers is the instability of their precursors, we also investigate the effects of iron sulfur and iron–copper sulfur minerals on the stability of ribooligonucleotides in formamide and in water. All of the iron sulfur and iron–copper sulfur minerals stimulated degradation of RNA. The relevance of these findings with respect to the origin of informational polymers is discussed.

Introduction

Plausible scenarios for the origin of life entail the robust prebiotic synthesis of informational polymers by condensation of simple chemical precursors.¹ Among the chemical precursors taken into consideration, the two related compounds hydrogen cyanide (HCN) and formamide (NH₂COH, **1**) have been the subject of thorough analyses.^{1,2} These compounds are easily converted by hydrolysis or dehydration. The attention given these two compounds is mainly due to their ability to synthesize nucleic bases under relatively mild experimental conditions coherent with those existing on the primitive Earth.³ It is noteworthy that formamide is the only chemical precursor able to synthesize at the same time, in addition to some amino acid derivatives, both purine and pyrimidine nucleic bases.⁴ In agreement with the hypotheses by Bernal⁵ and Cairns-Smith,⁶ the prebiotic chemistry of formamide is finely tuned by the

presence of different metal oxides and minerals in the reaction mixture,⁷ thus modeling the environment of the primitive Earth. These compounds can act as catalysts for condensation processes, enhancing the concentration of the reactant and preserving newly formed biomolecules from chemical and photochemical degradation.⁸ Moreover, minerals can catalyze the in situ decomposition of formamide to other chemicals that are potentially useful for the construction of both purine and pyrimidine scaffolds, such as ammonia and HCN.⁴ The effect of metal oxides and minerals on the chemistry of formamide has been studied in detail to better correlate the selectivity of the prebiotic syntheses to the chemical properties and elemental composition of the catalyst.² Metal oxides characterized by photoreactivity, such as titanium dioxide (TiO₂), are efficient catalysts for the synthesis of different nucleobases from formamide, accompanied by release of formaldehyde.⁹ This aldehyde, which is the main precursor of sugars through a formose-like condensation,¹⁰ provides, in addition to formamide, the optimal substrates for the first reported one-pot prebiotic synthesis of nucleoside derivatives. The possibility of synthesizing the sugar moiety directly on the formylated nucleobases by successive addition of one-carbon fragments opens novel

[†] Università della Tuscia.

[‡] Università Tor Vergata.

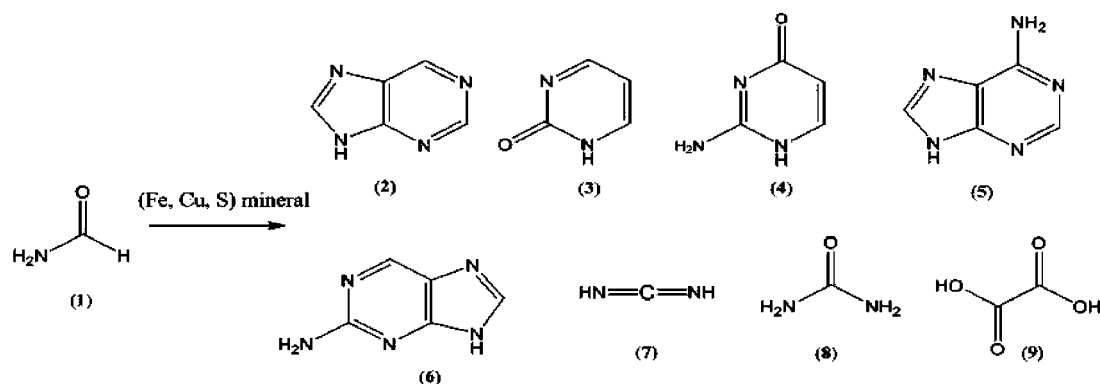
[§] Istituto di Biologia e Patologia Molecolari.

^{||} Università "Sapienza".

- (1) *Prebiotic Chemistry*; Walde, P., Ed.; Topics in Current Chemistry, Vol. 259; Springer-Verlag: Berlin Heidelberg, 2005.
- (2) For recent reviews, see: (a) Saladino, R.; Crestini, C.; Ciciriello, F.; Costanzo, G.; Negri, R.; Di Mauro, E. In *Astrobiology: Future Perspectives*; Ehrenfreund, P., Ed.; Kluwer: Dordrecht, The Netherlands, 2004; pp 393–413. (b) Saladino, R.; Crestini, C.; Ciciriello, F.; Costanzo, G.; Di Mauro, E. *Origins Life Evol. Biosphere* **2006**, *36*, 523–531.
- (3) Saladino, R.; Crestini, C.; Costanzo, G.; Di Mauro, E. In *Prebiotic Chemistry*; Walde, P., Ed.; Topics in Current Chemistry, Vol. 259; Springer-Verlag: Berlin Heidelberg, 2005; pp 29–68.
- (4) Saladino, R.; Crestini, C.; Ciambecchini, U.; Ciciriello, F.; Costanzo, G.; Di Mauro, E. *ChemBioChem* **2004**, *5*, 1471–1478.
- (5) Bernal, J. D. *The Physical Basis of Life*; Routledge and Kegan Paul: London, 1951.

- (6) Cairns-Smith, G. In *Possible Role for Minerals in Early Organisms*; Tran Tharh Van, J., Mounolou, J. C., Schneider, J., McKay, C., Eds.; Editions Frontières: Gif-sur-Yvette, France, 1992; pp 119–132.
- (7) Saladino, R.; Crestini, C.; Costanzo, G.; Negri, R.; Di Mauro, E. *Bioorg. Med. Chem.* **2001**, *9*, 1249–1253.
- (8) Saladino, R.; Crestini, C.; Costanzo, G.; Di Mauro, E. *Curr Org. Chem.* **2004**, *8*, 1425–1443.
- (9) Saladino, R.; Ciambecchini, U.; Crestini, C.; Costanzo, G.; Negri, R.; Di Mauro, E. *ChemBioChem* **2003**, *4*, 514–521.
- (10) (a) For a basic reference, see: Butlerow, A. *Ann. Phys.* **1861**, *120*, 296. (b) For a more recent reference, see: Decker, P.; Schweer, H.; Pohlman, R. *J. Chromatogr.* **1982**, *244*, 281–291.

Scheme 1



interesting scenarios for the prebiotic synthesis of nucleosides on the primitive earth.⁹

In a bottom-up approach to the synthesis of nucleic acids, the formation of nucleosides should be followed by their transformation to nucleotides. This can possibly be achieved by reaction of nucleosides with phosphate-containing minerals¹¹ following the release of the free phosphate necessary for the formation of the phosphoester bond as a result of the high dielectric constant of formamide.^{12,13}

Moreover, the iron content in a series of cosmic-dust analogues of terrestrial olivines, produced by laser ablation of simple oxides, finely tunes the selectivity of the reaction toward pyrimidine nucleic bases, with the yields of cytosine and uracil decreasing as a function of the content of iron in the mineral.¹⁴ Conversely, the yield of purine is unaffected by the elemental composition of the cosmic-dust analogues.

With the aim of further analyzing the effect of minerals on the prebiotic chemistry of formamide, we focused our attention on a family of iron sulfur minerals widely diffused on the primitive earth, such as pyrite (FeS_2) and pyrrhotine (Fe_{1-x}S). These minerals are key components in the Wächtershäuser hypothesis for the chemoautotrophic origin of the secondary metabolism,¹⁵ which is based on the formation of methyl mercaptan (CH_3SH) from carbon oxides (a primitive carbon-fixation pathway)¹⁶ in the presence of FeS and H_2S .¹⁷ Methyl mercaptan can be transformed into thioacetic acid, a plausible precursor of acetyl coenzyme A.¹⁸ In spite of the relevance of iron sulfur minerals in the primordial secondary metabolism, no data are available on their role in the origin of primary metabolic pathways, such as the synthesis of nucleic acids and their components. The study of this coupled scenario is

necessary to better define a primitive chemical system for the origin of life. Here we describe the role of different iron sulfur and iron–copper sulfur minerals in the prebiotic synthesis of nucleic bases and their components from formamide. In order to further evaluate the prebiotic role of these minerals, their effect on the stability of ribooligonucleotides was also determined.

Results

Iron Sulfur- and Iron–Copper Sulfur-Catalyzed Products of Formamide Condensation. We have selected a panel of original samples of pyrrhotine (Fe_{1-x}S), pyrite (FeS_2), chalcocopyrite (FeCuS_2), bornite (FeCu_3S_4), tetrahedrite [$(\text{Fe,Cu,Sb})\text{S}$] and covellite (CuS) as representative iron sulfur and iron–copper sulfur minerals differing in elemental composition. Commercially available iron sulfide FeS (synthetic pyrrhotine) and iron disulfide FeS_2 (synthetic pyrite) (Aldrich) were used as references. The reactions with pyrite and covellite were also performed by mixing the minerals in different amounts to evaluate the effect of more complex systems. As a general procedure, the syntheses were performed by heating pure formamide **1** (5 mL, 0.126 mol) at 160 °C for 48 h in the presence of catalytic amounts of the appropriate mineral (2% w/w). Yields were calculated as milligrams of product formed per gram of formamide. We focused on the characterization of the more abundant products by gas chromatography–mass spectrometry (GC–MS) analysis [after derivatization with *N,N*-bis(trimethylsilyl)trifluoroacetamide in pyridine] via comparison with authentic samples and, when necessary, by ¹H and ¹³C nuclear magnetic resonance (NMR) analysis of purified samples. In agreement with previously reported data, the condensation of **1** in the absence of minerals afforded purine as the only recovered product (~34.0 mg/g of formamide). The quantitative profile of nucleic acid components and other products obtained from formamide and iron sulfur and iron–copper sulfur minerals is reported in Scheme 1 and Table 1.

Initially, we evaluated the role of pyrrhotine and pyrite on the condensation of formamide. Heating formamide in the presence of pyrrhotine yielded a large panel of reaction products, including purine (**2**), 2(1H)-pyrimidinone (**3**), isocytosine (**4**), adenine (**5**), carbodiimide (**7**), and oxalic acid (**9**) (Scheme 1; Table 1, entry 1). Commercially available FeS showed similar behavior (Table 1, entry 2). Compounds **2**, **3**, **4**, and **7** were obtained in highest yield with both pyrite and FeS_2 (Table 1, entries 3 and 4). Moreover, pyrite showed a slightly different selectivity with respect to pyrrhotine, as 2-aminopurine (**6**) was also isolated in the reaction mixture in appreciable yield. Support is provided for the mechanism of formation of nucleobases from

(11) Ciciriello, F.; Costanzo, G.; Crestini, C.; Saladino, R.; Di Mauro, E. *Astrobiology* **2007**, *7*, 616–630.

(12) Saladino, R.; Crestini, C.; Neri, V.; Ciciriello, F.; Costanzo, G.; Di Mauro, E. *ChemBioChem* **2006**, *7*, 1707–1714.

(13) Costanzo, G.; Saladino, R.; Crestini, C.; Ciciriello, F.; Di Mauro, E. *J. Biol. Chem.* **2007**, *282*, 16729–16735.

(14) Saladino, R.; Crestini, C.; Neri, V.; Brucato, J. R.; Colangeli, L.; Ciciriello, F.; Di Mauro, E.; Costanzo, G. *ChemBioChem* **2005**, *6*, 1368–1374.

(15) (a) Wächtershäuser, G. *Syst. Appl. Microbiol.* **1988**, *10*, 207–210. (b) Wächtershäuser, G. *Proc. Natl. Acad. Sci. U.S.A.* **1990**, *87*, 200–204. (c) Wächtershäuser, G. *Prog. Biophys. Mol. Biol.* **1992**, *58*, 85–201.

(16) Fuchs, G.; Stupperich, E. In *Evolution of Prokaryotes*; Schleifer, K. H., Stackebrandt, E., Eds.; Academic Press: London, 1985; pp 235–251.

(17) Heinen, W.; Lauwers, A. M. *Origins Life Evol. Biosphere* **1996**, *26*, 131–150.

(18) Huber, C.; Wächtershäuser, G. *Science* **1997**, *276*, 245–247.

Table 1. Quantitative Profile of Products Obtained from Formamide and Iron- and Copper-Containing Minerals^a

entry	catalyst	yield (mg g ⁻¹) ^b							
		2	3	4	5	6	7	8	9
1	FeS ^c	0.50	0.17	0.01	0.01	—	0.01	—	0.01
2	pyrrhotine Fe _{1-x} S ^d	0.25	0.12	0.01	0.01	—	0.03	0.01	0.03
3	FeS ₂ ^e	3.00	0.55	0.50	0.11	0.15	0.30	0.10	—
4	pyrite FeS ₂ ^f	3.74	0.25	0.48	0.18	0.10	0.11	0.10	—
5	chalcopyrite FeCuS ₂ ^g	9.84	6.00	0.56	0.20	—	6.80	—	—
6	bornite FeCu ₅ S ₄ ^h	12.00	0.51	1.20	1.80	—	—	0.05	0.50
7	tetrahedrite (Fe,Cu,Sb)S ⁱ	37.44	2.85	0.82	0.19	—	0.22	0.20	—
8	covellite CuS ^j	—	5.80	0.06	—	—	0.32	—	0.50
9	covellite/pyrite (2:1)	2.20	0.02	0.02	0.01	—	0.20	—	0.02
10	covellite/pyrite (3:1)	3.75	0.19	0.04	—	—	0.21	0.03	0.02
11	covellite/pyrite (4:1)	4.12	0.94	0.27	0.02	—	0.07	0.02	—

^a Products were identified by comparison of their retention times and mass spectra with those of authentic samples. ^b Quantitative evaluations were performed by capillary gas-chromatographic analysis as described in Materials and Methods. Because of the uncertainty in the amounts of formamide involved in the synthesis of the recovered products, the yields were calculated as milligrams of product formed per gram of formamide. ^c Highly pure commercially available Fe_{1-x}S, where 0 < x < 0.2. ^d Natural source: mineral from China. ^e Highly pure commercially available FeS₂. ^f Mineral from Spain. ^g Mineral from Perú. ^h Mineral from Butte, MT. ⁱ Mineral from Perú. ^j Mineral from Butte, MT.

formamide,¹⁹ confirming the role of the decomposition products of formamide in the construction of the purine and pyrimidine scaffolds. To our knowledge, this is the first report of the ability of pyrrhotine and pyrite, which are usually connected with the origin of secondary metabolism, to catalyze the prebiotic synthesis of precursors of primary metabolism, such as purine and adenine, and of nucleobase isomers, such as isocytosine, 2-aminopurine, and 2(1*H*)-pyrimidinone.²⁰ The structure of isocytosine **4**, detected as the tris(silyl) derivative, was unambiguously assigned by gas-chromatographic comparison with an authentic sample. Isocytosine showed a significant difference in its retention time (*t_R*) value relative to that of cytosine, the isomer usually obtained during formamide condensation (Table 2).

Similarly, the monosilyl derivative of 2(1*H*)-pyrimidinone **3** showed a different value of *t_R* and a different pattern of the main fragmentation peaks than its isomer 4(3*H*)-pyrimidinone (Table 2).

Isocytosine [2-aminopyrimidin-4(3*H*)-one] is a structural isomer of cytosine and exists as two major tautomers. Although isocytosine is not a natural nucleobase like cytosine, nucleoside derivatives of isocytosine are valuable probes for studies of the formation of DNA triplex²¹ and mechanistic studies of RNA catalysis.²² Isocytosine can recognize guanine by a reversed Watson–Crick (RWC) interaction.²³ Moreover, the hydrogen-bonding pattern of the isocytosine/cytosine (iCC) pair is similar to that of the guanine/cytosine (GC) pair in both the RWC and the normal Watson–Crick interactions, the discrepancies in bond lengths and interaction energies being within 0.02 Å and 0.2 kcal/mol, respectively (Figure 1).²⁴ Thus, isocytosine could perform as bioisoster of guanine in the hydrogen-bonding interactions with natural nucleobases. Since guanine was never

synthesized from formamide, the formation of isocytosine with iron sulfur minerals opens a novel scenario in which the iCC pair might reproduce the extant-day GC interactions in primordial nucleic acids. Moreover, the synthesis of 2-pyrimidinone nucleosides from 2(1*H*)-pyrimidinone and ribose using the reaction conditions described by Orgel²⁵ has recently been reported as the first successful example of formation of the β-glycosidic bond between a pyrimidine base and an unactivated sugar in a plausible prebiotic reaction.²⁶

2-Aminopurine **6** is a purine-derivative isomer of adenine, the only difference with adenine being the position of the amino group. The structure of **6** was unambiguously assigned by comparison with an authentic sample. Ion peaks at *m/z* 207 and 135 were found to be specific markers for this compound (as opposed to adenine) in GC–MS analysis (Table 2). 2-Aminopurine can be incorporated into DNA during replication without inhibiting the base pairing in B-form DNA. Whereas adenine and 2-aminopurine normally pair with thymine, 2-aminopurine can also form a base pair with cytosine.²⁷ This implies that 2-aminopurine can produce AT/GC transitions in the next generation, generating transition mutations.²⁸

In order to further evaluate the role of minerals on the efficiency and selectivity of the condensation of formamide, we successively studied the catalytic activity of a series of (Fe,Cu)S minerals characterized by different elemental compositions, such as chalcopyrite (FeCuS₂), bornite (FeCu₅S₄), tetrahedrite [(Fe,Cu,Sb)S] and covellite (CuS). As shown in Scheme 1 and Table 1, condensation of formamide carried out in the presence of chalcopyrite, bornite, or tetrahedrite produced purine and adenine in higher yield than that using pyrrhotine or pyrite (Table 1, entries 5–7). In contrast, purine and adenine were not synthesized in the presence of covellite (Table 1, entry 8). Thus, the presence of iron in the elemental composition of the mineral was a crucial factor for the synthesis of purine derivatives, except in the case of 2-aminopurine, which was obtained only in the presence of pyrite.

(19) Saladino, R.; Crestini, C.; Ciciriello, F.; Costanzo, G.; Di Mauro, E. *Chem. Biodiversity* **2007**, *4*, 694–720.

(20) When some of our experiments on the condensation of formamide were revisited, low amounts of the nucleobase isomers isocytosine and 2(1*H*)-pyrimidinone were also detected in the presence of mineral phosphates and clays.

(21) Ono, A.; Ts'o, P. O. P.; Kan, L. *J. Am. Chem. Soc.* **1991**, *113*, 4032–4033.

(22) Oyelere, A. K.; Kardon, J. R.; Strobel, S. A. *Biochemistry* **2002**, *41*, 3667–3675.

(23) Gupta, D.; Huelsekopf, M.; Cerdà, M. M.; Ludwig, R.; Lippert, B. *Inorg. Chem.* **2004**, *43*, 3386–3393.

(24) Zhanpeisov, N. U.; Leszczynski, J. *THEOCHEM* **1999**, *487*, 107–115.

(25) Fuller, W. D.; Sanchez, R. A.; Orgel, L. E. *J. Mol. Evol.* **1972**, *1*, 249–257.

(26) Bean, H. D.; Sheng, Y.; Collins, J. P.; Anet, F. A. L.; Leszczynski, J.; Hud, N. V. *J. Am. Chem. Soc.* **2007**, *129*, 9556–9557.

(27) Sowers, L. C.; Boulard, Y.; Frazier, G. V. *Biochemistry* **2000**, *39*, 7613–7620.

(28) Ramaekers, R.; Adamowicz, L.; Maes, G. *Eur Phys. J. D* **2002**, *20*, 375–388.

Table 2. Selected Mass Spectrometric Data of Condensation Products **2–14**^a

products	<i>t_R</i> (min) ^e	<i>m/z</i> (%)
2(1 <i>H</i>)-pyrimidinone ^b	6.6	168 (25) [M], 153 (100) [M-CH ₃], 123 (3) [M-(CH ₃) ₃]
4(3 <i>H</i>)-pyrimidinone ^b	4.9	168 (20) [M], 167 (17) [M-H], 153 (100) [M-CH ₃], 123 (3) [M-(CH ₃) ₃]
purine ^b	11.0	192 (79) [M], 177 (100) [M-CH ₃], 120 (10) [M-Si(CH ₃) ₃]
isocytosine ^d	11.8	327 (18) [M], 312 (100) [M-CH ₃], 282 (1) [M-(CH ₃) ₃], 255 (6) [M-H-Si(CH ₃) ₃], 240 (7) [M-H-Si(CH ₃) ₃ -CH ₃], 182 (2) [M-(Si(CH ₃) ₃) ₂]
cytosine ^c	11.2	255 (49) [M], 254 (100) [M-H], 240 (72) [M-CH ₃], 182 (5) [M-H-Si(CH ₃) ₃]
adenine ^c	15.3	279 (27) [M], 264 (100) [M-CH ₃], 249 (1) [M-(CH ₃) ₂], 192 (17) [M-Si(CH ₃) ₃]
2-aminopurine ^c	15.6	279 (20) [M], 264 (100) [M-CH ₃], 249 (2) [M-(CH ₃) ₂], 207 (15) [M-Si(CH ₃) ₃], 192 (80) [M-Si(CH ₃) ₃ -CH ₃], 135 [M-(Si(CH ₃) ₃) ₂]
carbodiimide ^c	3.70	186 (14) [M], 171 (100) [M-CH ₃], 141 (4) [M-(CH ₃) ₃], 113 (2) [M-Si(CH ₃) ₃], 98 (11) [M-Si(CH ₃) ₃ -CH ₃], 83 (2) [M-Si(CH ₃) ₃ -(CH ₃) ₂]
urea ^c	7.50	204 (3) [M], 189 (59) [M-CH ₃], 147 (100) [M-Si(CH ₃) ₂], 131 (5) [M-Si(CH ₃) ₃], 116 (2) [M-NH-Si(CH ₃) ₃], 88 (2) [M-CO-NH-Si(CH ₃) ₃], 73 (55) [M-CO-NH-Si(CH ₃) ₃ -CH ₃]
oxalic acid ^c	5.70	219 (3) [M-CH ₃], 189 (5) [M-(CH ₃) ₃], 147 (78) [M-Si(CH ₃) ₃ -CH ₃], 117 (1) [M-Si(CH ₃) ₃ -3CH ₃], 73 (100) [M-(Si(CH ₃) ₃) ₂ -O]

^a Mass spectroscopy was performed by using a GC-MS QP5050A instrument. Samples were analyzed after treatment with *N,N*-bis(trimethylsilyl)trifluoroacetamide and pyridine. ^b Product analyzed as the monosilyl derivative. ^c Product analyzed as the bis(silyl) derivative. ^d Product analyzed as the tris(silyl) derivative. ^e Analytical tools are described in Materials and Methods.

These data are in agreement with the effect of the iron content on the catalytic activity of cosmic-dust analogues.¹⁴ Irrespective of the experimental conditions, all of the (Fe,Cu)S minerals catalyzed the synthesis of isocytosine and 2(1*H*)-pyrimidinone in moderate to high yields, with chalcopyrite and tetrahedrite being the best catalysts (Table 1, entries 5–8).

In regard to the selectivity in the synthesis of compounds **7–9**, no generalized trend can be identified, given that none of the minerals performed uniformly better than the others. However, optimized conditions can be identified for each product, allowing the considerably enhanced yields reported above for pyrite and pyrrothine. As an example, chalcopyrite was the best catalyst for **7** and tetrahedrite the best for **8**, while both bornite and covellite were most effective for **9**. The synthesis of carbodiimide **7**, which is an important activating

agent for the condensation of amino acids into peptides and of nucleotides into oligonucleotides,²⁹ is most probably due to water elimination from newly formed urea.

This hypothesis is in agreement with the presence of traces of carbodiimide observed during the GC-MS analysis of an authentic sample of urea used as a standard for quantitative determinations. Thus, urea, which participates as a basic building block in the construction of both purine and pyrimidine scaffolds, can also play the role of a generator of activating agents for the polymerization of low-molecular-weight biomolecules.³⁰

In the Wächtershäuser experiments, mixtures of iron-sulfur minerals were also used as model of the complex environment of the primitive earth. As an example, pyrrothine and nickel sulfide (NiS), which coexist in the crystal structure of pentlandite, were mixed in order to better tune the redox properties of the system. In view of these considerations, we performed an additional series of experiments using a mixture of the simplest metal sulfides, pyrite and covellite (with pyrite/covellite ratios ranging from 1:2 to 1:4 w/w). As shown in Table 1, the yield of purine increased as the amount of covellite in the reaction mixture increased, while only a low yield of adenine was observed irrespective of the experimental conditions. In the case of pyrimidines, the yields of both 2(1*H*)-pyrimidinone and isocytosine increased as the amount of covellite increased, with a more pronounced effect for pyrimidinone. It should be noted that the yield of pyrimidine derivatives recovered with mixtures of covellite and pyrite was lower than that previously obtained with pyrite alone, suggesting a major role for this mineral in the construction of the pyrimidine scaffold. On the basis of these data, even though the main catalytic properties of covellite and pyrite were retained in the mixtures, specific synergisms between these two catalysts were not observed.

The role of water in prebiotic synthetic processes is a controversial topic. Even though water is supposedly the environment in which life originated, chemical precursors such as hydrogen cyanide and formamide are actively degraded in water, where their concentrations rapidly decrease and the synthesis of biomolecules necessary for the origin of the initial informational polymers is thermodynamically impaired. As an example, formamide is hydrolyzed by water to ammonium formate with a half-life (*t*_{1/2}) of nearly 200 years at 25 °C (*k*_w = 1.1 × 10⁻¹⁰ s⁻¹ at 25 °C), and the rate of hydrolysis increases with the reaction temperature and the acidity of the medium.³¹

Hence, an evaluation of the effect of water in prebiotic synthetic processes from formamide is relevant. Experiments were thus performed in which the condensation of formamide on pyrite was analyzed in the presence of different amounts of water. As shown in Table 3, appreciable amounts of compounds **2–7** were recovered in the presence of 20 wt % water. Purine, isocytosine, and carbodiimide were also recovered in reaction mixtures containing up to 30 wt % water. Finally, only purine and carbodiimide were observed in the presence of 40 wt % water.

On the basis of these data, it may be concluded that the condensation of formamide can work in mixed formamide/water solutions. Moreover, formamide has a boiling point of 210 °C

- (29) Hartmann, J.; Nawroth, T.; Dose, K. *Origin Life* **1984**, *14*, 213–218.
 (30) (a) Eschenmoser, A.; Loewenthal, E. *Chem. Soc. Rev.* **1992**, *21*, 1–16. (b) Sanchez, R.; Ferris, J. P.; Orgel, L. E. *Science* **1966**, *153*, 72–73. (c) Orgel, L.; Lohmann, R. *Acc. Chem. Res.* **1974**, *7*, 368–377.
 (31) Slebocka-Tilk, H.; Sauriol, F.; Monette, M.; Brown, R. S. *Can. J. Chem.* **2002**, *80*, 1343–1350.

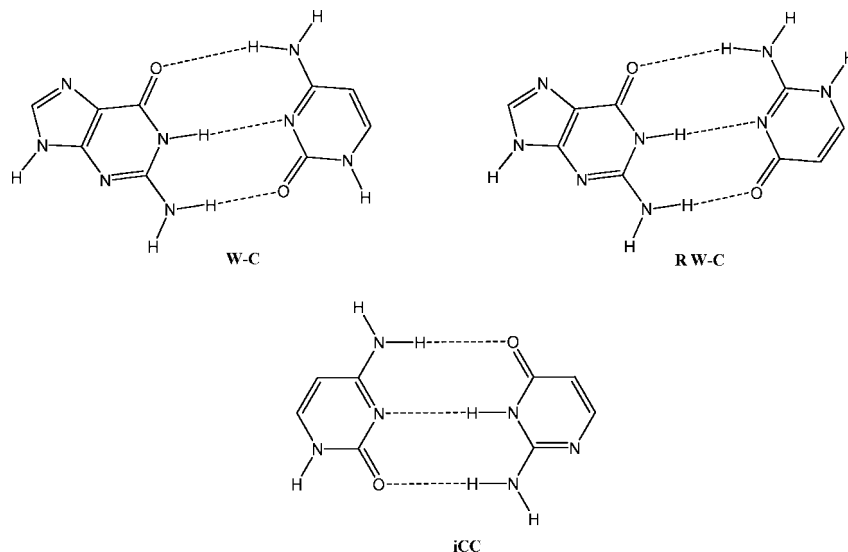


Figure 1. Isocytosine ability in Watson–Crick and reversed Watson–Crick interactions. W-C: guanine–cytosine pair. R W-C: reversed guanine–isocytosine pair. iCC: cytosine–isocytosine pair.

Table 3. Quantitative Profile of Products from Formamide and Pyrite in the Presence of Water^a

entry	wt % H ₂ O ^b	yield (mg g ⁻¹) ^{c,d}						
		2	3	4	5	7	8	9
1	0	0.25	3.74	0.08	0.18	0.11	0.10	—
2	10	0.05	2.00	0.02	0.04	0.06	—	—
3	20	0.02	1.33	0.01	0.01	0.04	—	0.01
4	30	0.02	0.20	—	—	0.02	—	—
5	40	0.03	—	—	—	0.02	—	—

^a Products were identified by comparison of their retention times and mass spectra with those of authentic samples. ^b The reactions were performed using the percentage of water reported in the table and 2% pyrite (w/w relative to formamide). ^c Quantitative evaluations were performed by capillary gas-chromatographic analysis as described in Materials and Methods. ^d Ammonium formate (HCOONH₄) produced by hydrolysis of formamide was recovered by sublimation of the reaction mixture.

with a very limited azeotropic effect and thus can easily be concentrated by water evaporation in a dry-lagoons model.³²

Effects of Iron Sulfur Minerals on the Stability of Phosphoester Bonds. Formamide is both a precursor for the synthesis of nucleobases and an active degrading agent of DNA³³ and RNA.³⁴ The commonly accepted “RNA world” scenario entails the origin of informational polymers from RNA or RNA-like (pre)genetic polymers. We have determined the effects of the iron sulfur minerals on water- and formamide-based nucleic acid degradation, focusing on RNA. The conditions tested are comparable with those that afforded the syntheses described here.

The panel of minerals analyzed in this study were tested for their ability to interfere with the degradative process of ribonucleotide oligomers. RNA oligonucleotides are cleaved according to a well-characterized mechanism.^{34,35} The cleavage of the phosphoester chain normally requires participation of the

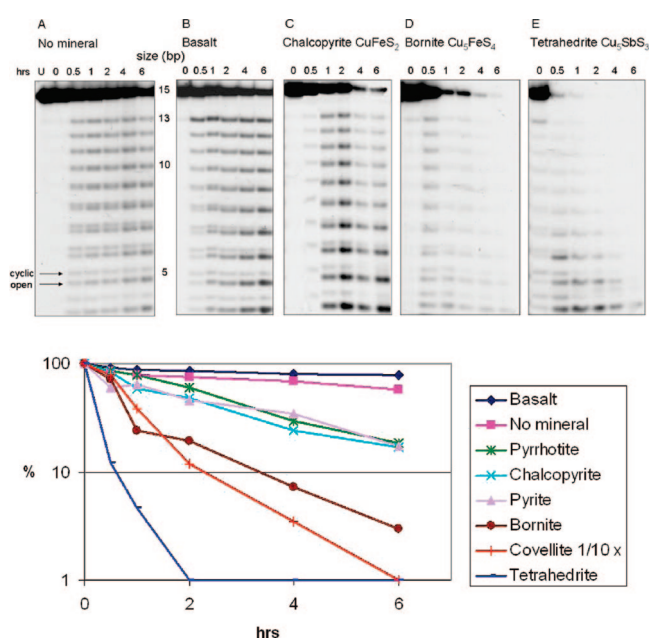


Figure 2. Iron sulfur minerals modify the degradative reaction of RNA in formamide. (top) Degradation profiles of the 5′-labeled 5′-AAAAAAAAAAAAAU-3′ ribooligomer in the (A) absence or (B–E) presence of a mineral (as indicated above each profile). The reactions were performed for the indicated times under the conditions described in Materials and Methods. The size of the resulting fragments is indicated to the right of the profile A. (bottom) Kinetics of degradation of the oligomer in the absence or presence of the indicated minerals, reported as the percentage of the full-sized molecule (ordinate) as a function of the reaction time (abscissa).

2′-OH group as an internal nucleophile³⁴ in two “nucleophilic cleavage” events: the transesterification reaction and the hydrolysis reaction. During transesterification, the 2′-OH nucleophile attacks the tetrahedral phosphorus to afford a 2′,3′-cyclic monophosphate. This species is then hydrolyzed into a mixture of 3′- and 2′-phosphate monoesters. Both steps are catalyzed by protons, hydroxide, nitrogen derivatives, and metal ions.

The degradation kinetics of 5′-labeled RNA oligomers treated at 80 °C in formamide and in water are reported in Figures 2 and 3, respectively, in the absence and presence of the iron sulfur minerals studied.

(32) Formic Acid and Derivatives. *Kirk-Othmer Encyclopedia of Chemical Technology*, 3rd ed.; John Wiley & Sons: New York, 1978.

(33) Negri, R.; Ferraboli, S.; Barlati, S.; Di Mauro, E. *Nucleic Acids Res.* **1994**, *22*, 111–112.

(34) Morrow, J. R.; Aures, K.; Epstein, D. *J. Chem. Soc. Chem. Commun.* **1995**, *23*, 2431–2432.

(35) Saladino, R.; Crestini, C.; Ciciriello, F.; Di Mauro, E.; Costanzo, G. *J. Biol. Chem.* **2006**, *281*, 5790–5796.

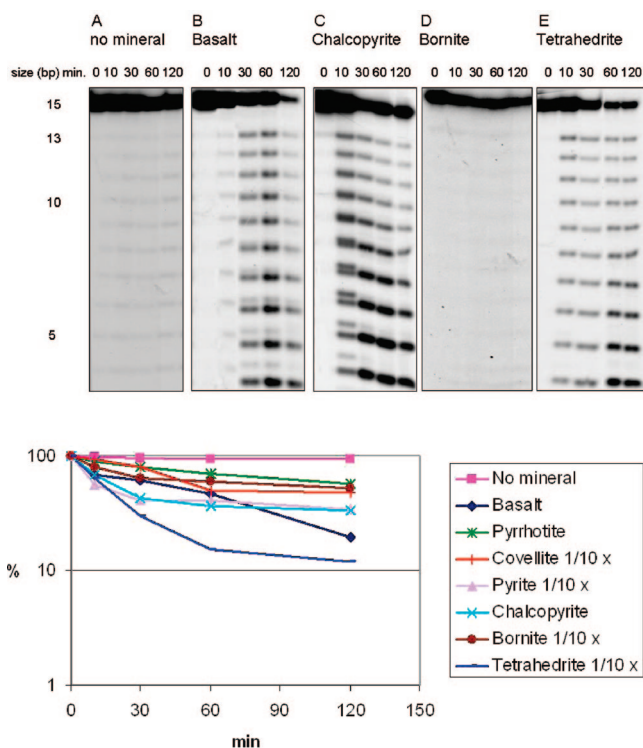


Figure 3. Iron sulfur minerals modify the degradative reaction of RNA in water. The descriptions of the top and bottom panels are the same as in Figure 2.

RNA Degradation by Formamide. The kinetics of RNA degradation by pure formamide is shown in Figure 2. The top panel shows selected examples of degradation profiles, as obtained in the presence of the indicated minerals: basalt, chalcopyrite, bornite, and tetrahedrite. The degradation profile characteristically yields a double-banded profile because a first cleavage of the 5' phosphodiester bond leaves a 2'–3' cyclic phosphate extremity³⁶ that is successively opened, resulting in a 2' or 3' phosphate extremity (as indicated to the left of profile A). The graph in the bottom panel reports the kinetic evaluation of the degradation profiles observed for the minerals listed above as well as for pyrrhotine, pyrite, and covellite, which produced similar profiles (not shown). The protective effect by basalt is evident, while all of the iron sulfur and iron–copper sulfur minerals stimulated degradation in the following order ($t_{1/2}$ values (min) given in parentheses): covellite (1.8) > tetrahedrite (5.4) > bornite (0.17×10^2) > pyrite (0.25×10^2) > chalcopyrite (0.46×10^2) > pyrrhotine (0.58×10^2) > basalt (1.08×10^3). The half-life of the 15-mer oligonucleotide in formamide at 80 °C in the absence of minerals is 0.4×10^3 min. These data are in accordance with the effect of Fe^{2+} salts to induce site-specific cleavage of different RNAs at neutral pH.³⁶ In this latter case, the possible role of metal-dependent redox process on the cleavage of the internucleotide bonds is suggested by the mechanism of the phosphoryl transfer from a diiron oxo protein (from porcine uterus), where two iron ions in both +2 and +3 oxidation states are involved in the catalytic cycle.³⁷

RNA Degradation by Water. The kinetics of RNA degradation in water is shown in Figure 3. The organization of this

figure and the description of its data are the same as in Figure 2. In water, the degradative effect exerted by the minerals is stronger, and the half-lives of the oligomers in their presence are correspondingly shorter. The kinetics of RNA oligomer hydrolysis in pure water is known in detail.^{38,39} The order of the degradative effect ($t_{1/2}$ values (min) in parentheses) is as follows: tetrahedrite (2.00) > pyrite (2.10) > covellite (6.60) > chalcopyrite (0.26×10^2) > basalt (0.58×10^2) > bornite (1.52×10^2) > pyrrhotine (1.80×10^2). The half-life of the 15mer oligonucleotide in water at 80 °C in the absence of minerals is $>5 \times 10^2$ min.

In summary, analysis of the stability of RNA in iron sulfur minerals revealed the marked enhancement of the degradation process by these compounds.

Discussion

Formamide affords a large number of nucleic bases and related compounds in the presence of iron sulfur minerals. The syntheses occur relatively quickly and under moderate conditions in the presence of each of the minerals tested. Taken together with the reported syntheses occurring under similar conditions from formamide in the presence of a large variety of other catalysts (i.e., silica, alumina, zeolites, CaCO_3 , TiO_2 , common clays, kaolin, montmorillonites, olivines and their cosmic-dust analogues, and phosphate minerals, as reviewed in ref 2), these data show the strong intrinsic ability of formamide to condense into prebiotically relevant compounds. Iron sulfur minerals are usually involved as catalysts in the Wächtershäuser hypothesis for the chemoautotrophic origin of key components of primordial secondary metabolism, such as thioacetic acid, a possible ancestor of acetyl coenzyme A. The evidence that the same minerals can catalyze the condensation of formamide to nucleobases and related isomers opens novel scenarios for a synthetic machinery able to simultaneously synthesize compounds useful for the origin of primary and secondary metabolism.

On the other hand, can iron sulfur minerals be considered a preferential class of catalysts in a prebiotic scenario relative to other classes of minerals? From this perspective, considerations of the stability of pregenetic materials are particularly relevant.

The syntheses of nucleobases from formamide and their formamide-based phosphorylation¹³ would remain a biologically useless series of events if the eventually formed polymers were not under thermodynamic conditions allowing their survival as macromolecules. In this respect, sets of physicochemical conditions have been identified under which the polymeric state of phosphorylated nucleotides is favored over the monomeric one for both ribo-³⁵ and deoxyribonucleotide⁴⁰ systems. However, the thermal and chemical ranges of the reported conditions are small, and the protective effect is limited.^{35,40}

In this frame of reference, the following question applies: do the minerals that catalyze the syntheses of nucleic bases exert a protective effect on the polymers that would possibly form in their environment? Protective effects on ribonucleotides have been reported for clays^{4,41,42} and phosphate minerals.^{11,12} The data reported here show that iron sulfur minerals go in the

(38) Soukup, G.; Breaker, R. *RNA* **1999**, *5*, 1308–1325.

(39) Ciciriello, F.; Costanzo, G.; Pino, S.; Crestini, C.; Saladino, R.; Di Mauro, E. *Biochemistry* **2008**, *47*, 2732–2742.

(40) Saladino, R.; Crestini, C.; Busiello, V.; Ciciriello, F.; Costanzo, G.; Di Mauro, E. *J. Biol. Chem.* **2005**, *280*, 35658–35669.

(41) Biondi, E.; Branciamore, S.; Fusi, L.; Gago, S.; Gallori, E. *Gene* **2007**, *389*, 10–18.

(42) Biondi, E.; Branciamore, S.; Maurel, M. C.; Gallori, E. *BMC Evol. Biol.* **2007**, *7* (Suppl. 2), S2.

(36) Vary, C. P. H.; Vournakis, J. N. *Proc. Natl. Acad. Sci. U.S.A.* **1984**, *81*, 6978–6982.

(37) David, S. S.; Que, L. *J. Am. Chem. Soc.* **1990**, *112*, 6455–6463.

opposite direction and that if polymers had to endure their presence, ancillary mechanisms (e.g., encapsulation in lipids, interaction with protective surfaces, aggregation and/or precipitation, rapid removal, etc.) must have been contemporaneously active.

Materials and Methods

Formamide (Fluka, >99%) and betulinol (Aldrich) were used without further purification. Gas-chromatographic and mass-spectrometric analyses were performed with an HP5890 II gas chromatograph and a Shimadzu GC-MS QP5050A equipped with an Varian CP8944 column (column type, WCOT fused silica; film thickness, 0.25 μm ; stationary phase, VF-5ms; ϕ , 0.25 mm; length, 30 m). Samples were analyzed after treatment with *N,N*-bis(trimethylsilyl)trifluoroacetamide and pyridine. ^1H and ^{13}C NMR spectra were recorded on a Bruker (200 MHz) spectrometer and are reported in δ value. Microanalyses were performed with a Carlo Erba 1106 analyzer. Chromatographic purifications were performed on columns packed with Merck silica gel, 230–400 mesh for flash technique. TLC was carried out using Merck platten Kieselgel 60 F₂₅₄.

General Procedure for Formamide Condensation. Formamide (5.7 g, 5 mL, 0.12 mmol) was heated at 160 °C for 48 h in the presence of the appropriate mineral (2% w/w): pyrrhotine (Fe_{1-x}S), pyrite (FeS₂), chalcopyrite (FeCuS₂), bornite (FeCu₅S₄), tetrahedrite (Fe,Cu,Sb)₃S, or covellite (CuS). The minerals were obtained from Ezio Curti (former provider and consultant for the Collection of Minerals of the Department of Mineralogy, University La Sapienza, Rome). Pure crystals were isolated under a microscope, washed twice (first with ethanol, then with analytical-grade distilled water), air-dried, and manually ground in a ceramic mortar.

The origins of the minerals are as follows: pyrrhotine, China; pyrite, Spain; chalcopyrite, Perú; bornite, Butte, MT; tetrahedrite, Perú; covellite, Butte, MT; basalt, Italy. Commercially available iron sulfide FeS (synthetic pyrrhotine) and iron disulfide FeS₂ (synthetic pyrite) (both obtained from Aldrich) were used as references. The reaction mixture was cooled, filtered to remove the catalyst, and evaporated under high vacuum. GC-MS analysis of a portion of the crude reaction mixture was performed using an isothermal temperature profile of 100 °C for the first 2 min followed by a 10 °C/min temperature gradient to 280 °C and finally an isothermal period at 280 °C for 40 min. The injector temperature was 280 °C. Chromatography-grade helium was used as the carrier gas. The fragmentation patterns were compared with those of authentic samples. Betulinol was used as an internal standard. When necessary, the crude reaction mixture was also purified by flash chromatography (9:1 CHCl₃/CH₃OH) and the structures of isolated products were confirmed with the usual spectroscopic techniques and by comparison with authentic commercial samples.

Selected spectroscopic data for isomers of natural nucleobases:

Isocytosine (4). Mp: 275 °C. ^1H NMR (DMSO-*d*₆) δ (ppm): 7.42 (3H, s, NH, NH₂), 7.20 (1H, d, *J* = 7.43 Hz, CH), 5.62 (1H, d, *J* = 7.43 Hz, CH). ^{13}C NMR (DMSO-*d*₆) δ (ppm): 171.07 (C=O), 150.06 (C), 131.79 (CH), 110.2 (CH). MS: *m/z* 111 (M⁺).

2-Aminopurine (6). Mp: 280–282 °C. ^1H NMR (D₂O + DCl) δ (ppm): 8.89 (1H, s, CH), 8.58 (1H, s, CH), 8.30 (3H, s, NH, NH₂). ^{13}C NMR (D₂O + DCl) δ (ppm): 160.6 (C), 155.11 (C), 147.7 (CH), 141.61 (CH), 125.51 (C). MS: *m/z* 135.13 (M⁺).

Degradation and Protection Analyses of Ribooligomers. The degradation of ribonucleotides in formamide and in water was studied using the 15-mer 5'-AAAAAAAAAAAAAU-3', purchased from Dharmacon Inc. (Chicago, IL).

RNA Preparation and 5' Labeling. P1 RNA (10 μmol) was labeled with [γ -³²P]ATP using polynucleotide kinase (Roche Applied Science). The oligomer was then purified on a 16% denaturing acrylamide gel (19:1 acrylamide/bisacrylamide). After elution, the residual polyacrylamide was removed by a NuncTrap Probe purification column (Stratagene). Two picomoles of RNA (typically 30 000 cpm) was processed for each sample.

Ribooligonucleotide Degradation Protocols and Analyses. The 5'-labeled oligonucleotide was treated at 80 °C under the time and solution conditions indicated where appropriate. A typical assay consisted of 15 μL of a solution containing 1 μL of RNA solution, 1 μL of mineral (as a 0.1 mg/ μL suspension of ground material), and 13 μL of water (pH 6.1) or formamide. Covellite in formamide and covellite, pyrite, bornite, and tetrahedrite in H₂O were particularly active and were also analyzed at 0.01 mg/ μL (as reported in Figures 2 and 3, respectively). This concentration was selected following a preliminary titration assay. To stop the reaction, a 5×10^{-4} M (final concentration) aqueous solution of tetrasodium pyrophosphate (Sigma) (pH 7.5) was added to a final volume of 40 μL . The samples were vortexed for 1 min and then centrifuged at 13 000 rpm for 20 min. This procedure was performed twice. The supernatant was ethanol-precipitated, resuspended in 5 μL of formamide buffer, heated for 2 min at 65 °C, and loaded on a 16% denaturing polyacrylamide gel (19:1 acrylamide/bisacrylamide). For these methods, see also refs 4 and 32.

The half-life of the oligonucleotide was determined using the standard graphical procedure from plots of the percent disappearance of the intact 15-mer molecules as a function of time. Disappearance was determined by densitometric analysis of the intensity of the full-length molecule in low-exposure autoradiograms. The sequence 5'-AAAAAAAAAAAAAU-3' was used in this study (instead of the apparently more logical use of a homogeneous polyA oligomer) because we had empirically observed that the ApU step in the 3' terminal position is cleaved with a much lower frequency than average. This behavior facilitated the quantitative evaluation of the 15-mer, which was not contaminated by the close presence of a 14-mer.

The quality of the gel electrophoretic images is not particularly high. This is due to the short size of the oligomer; in RNA analyses, longer fragments yield sharper images but complicate the analysis of the kinetics of the minerals in water.

Acknowledgment. This work was funded by the Italian Space Agency "MoMa Project", ASI-INAF n. I/015/07/0 "Esplorazione del Sistema Solare", and the U.S. National Science Foundation (CBC Program).

JA804782E